PIBB 生物化学与生物物理进展
Progress in Biochemistry and Biophysics
2016, 43(9): 895~902
www.pibb.ac.cn

Characterization of Photosystem Ⅰ and Photosystem Ⅱ From Spinach: Effect of Ionic Strength and Impact on Purification*

WANG Ling-Ling, HUANG Ya-Qi, ZHANG Xue-Fang, QU Jian-Bo, LIU Jian-Guo**
(*Center for Bioengineering and Biotechnology, China University of Petroleum (East China), Qingdao* 266580, China)

Abstract Our previous work has demonstrated that ultrafiltration has the potential for the isolation of photosystem Ⅰ (PSⅠ) from spinach at a large scale. In order to develop a practical bioseparation process, the "product" and the "impurity" should be characterized in order to select suitable membrane and optimize the operational and physiochemical parameters. One easily adjusted but critically important parameter, the solution ionic strength, and its effects on the properties of target protein (PSⅠ) and the major impurity (photosystem Ⅱ, PSⅡ) were studied. Following the isolation of PSⅠ and PSⅡ from spinach, the aggregation size, zeta potential, atomic force microscopy imaging and thermal stability were determined. Solution ionic strength was found to have a significant influence on the activity, aggregation size and thermal stability of both PSⅠ and PSⅡ. The results also demonstrated that the "molecular sieve effect" played a central role in the newly developed ultrafiltration process for PSⅠ isolation.

Key words photosystem Ⅰ, photosystem Ⅱ, ionic strength, characterization, purification
DOI: 10.16476/j.pibb.2016.0006

Photosystem Ⅰ (PSⅠ) and photosystem Ⅱ (PSⅡ) are membrane proteins which have chlorophyll-containing reaction centers found in thylakoid membranes of oxygenic photosynthetic organisms. The former uses the light energy to oxidize plastocyanin and reduce ferredoxin, while the latter is responsible for the light-driven transfer of electrons from water to plastoquinone [1]. To understand the molecular details of this machinery, photosystems (PSⅠ and PSⅡ) are needed in purified form and in large quantity to allow a detailed analysis by biophysical methods [2]. The separation has been challenging because of structural complexity and delicacy and the need for quick separation due to their inherent instability. However, the conventional techniques used for membrane protein purification, such as chromatography and sucrose density gradient centrifugation, suffer from long time-consuming processes and difficulties associated with scale up [3]. Therefore, the lack of enough quantities of photosystems has significantly impeded fundamental research on photosystems and limited their applications[4].

In our previous work, a novel membrane-based process was developed to isolate PSⅠ from spinach[5]. The results showed that the purity of PSⅠ obtained was about 84% after ultrafiltration and the activity recovery of PSⅠ was greater than 94%. In order to get a higher purity of PSⅠ and more importantly to develop a practical and scalable bioseparation process, key physiochemical properties of photosystems (PSⅠ and PSⅡ) and their dependence on operational

*This work was supported by grants from The National Natural Science Foundation of China (21276280, 21473256, 21176257) and Innovation Project of China University of Petroleum (YCXJ 2016042).
**Corresponding author.
Tel: 86-532-86981566, E-mail: jianguoliu@upc.edu.cn
Received: January 8, 2016 Accepted: September 1, 2016

parameters must be determined[6].

In this work, the effects of solution ionic strength on properties of PSⅠ and PSⅡ were examined after they were isolated from spinach and stabilised using *n*-dodecyl-beta-D-maltoside as detergent. The parameters studied here included the aggregation size, zeta potential and thermal stability, which are related to the mechanisms of membrane bioseparation process and membrane fouling. On the basis of our results, the mechanism of the novel membrane-based process for PSI isolation was proposed and validated, and new measures for further optimization of operating parameters were also developed.

1 Materials and methods

1.1 Materials

Fresh spinach was purchased from a local supermarket. *n*-dodecyl-beta-D-maltoside (DDM), methylviologen (MV), 3- (3, 4-dichlorophenyl)-1, 1-dimethylurea (DCMU), 2, 6-dichloroindophenol (DCIP), phenylmethane-sulfonyl fluoride (PMSF), ethylenediaminetetraacetate (EDTA), sucrose, and sorbitol were obtained from Sigma-Aldrich. Magnesium chloride, calcium chloride, sodium chloride, hydrochloric acid and other chemicals were purchased from Sinopharm Chemical Reagent Corporation and were of analytical or higher grade.

1.2 Preparation of PSⅠ and PSⅡ

The PSⅠ and PSⅡ were extracted from spinach according to the methods described by Bruce[7] and Liu *et al*[3], respectively. The chlorophyll contents of final purified PSⅠ and PSⅡ were measured as described previously[5]. All the purification steps of PSⅠ and PSⅡ were carried out in the dark at 4℃.

1.3 Low-temperature fluorescence measurements

Low-temperature fluorescence spectra of PSⅠ/PSⅡ samples were measured at an excitation wavelength of 436 nm using a Hitachi F-2500 Fluorescence Spectrofluorometer (Tokyo, Japan) with a slit setting of 2 nm. Each slide was cooled under liquid nitrogen in a cryostat and the fluorescence emission spectra were recorded from 600 nm to 800 nm. PSⅠ/PSⅡ samples prepared by normalizing chlorophyll concentrations (8 ～10 mg/L) were diluted to 50% glycerol and the path-length of cell was 6 mm. The fluorescence intensity of each sample was normalized to the integral over the wavelength shown.

1.4 PSⅠ/PSⅡ activity measurements

PSⅠ/PSⅡ activity measurements were performed according to the method of Liu *et al*.[5] using an O_2 electrode (Chlorolab2, Hansantech, U.K.). The working solution had a total volume of 1.01 ml. For PSⅠ assay, the solution contained 10 μmol/L DCMU, 0.1 mmol/L DCIP, 0.167 mmol/L MV, 1 mmol/L sodium ascorbate, and 1 mmol/L sodium azide. The Chl *a* concentration in the final solution was 10 mg/L. As for PSⅡ, the solution was changed to 400 mmol/L sucrose, 15 mmol/L NaCl, 20 mmol/L MES, 2 mmol/L $MgCl_2$, and 50.5 μg Chl *a*. A combination of 0.3 mmol/L DCBQ and 5 mmol/L $K_3[Fe(CN)_6]$ was used as an artificial electron acceptor. The electrode was standardized before and after each of the measurements with air saturated water according to the manufacturer's specifications. A fiber optic illuminator with lamp power 100 W and luminous intensity of 1 800 $\mu mol \cdot m^{-2} \cdot s^{-1}$ was used as a light source. All measurements were performed at 20℃ in 2.5 ml of liquid-phase electrode chamber under continuous stirring.

1.5 Atomic force microscopy (AFM) imaging

AFM images were collected using a Nanoscope Ⅳa (Vecco/Digital Instruments, Santa Barbara, CA, U.S.A.) operating in tapping mode. Soft silicon probes were used with tip radius of <10 nm mounted on a single-beam cantilever. PSⅠ/PSⅡ sample (2 μl, Chl *a* concentration was 50 mg/L) was deposited on a freshly cleaved mica surface for 1 min prior to rinsing 10 times with Milli-Q water (resistivity: 18.2 MΩ·cm, 25℃) to remove the buffer. After drying in a gentle stream of nitrogen gas, the AFM images were acquired immediately. Cantilever deflections were recorded with a cantilever frequency of 250 Hz, horizontal scan rate of 1.2 Hz and 512 samples for per line. Imaging was performed at 20℃ and the images were analyzed by Nanoscope software (Version 5.12r3).

1.6 Zeta potential measurement

Measurement of zeta potential of PSⅠ/PSⅡ complex were carried out with a Zetasizer Nano-ZS (Malvern Instruments, U.K.). Prior to the measurement, each sample was centrifuged at 2 000 *g* for 10 min to remove the visible particles. The Chl *a* concentration in PSⅠ/PSⅡ solution was 50 mg/L. The analysis was conducted at 4℃. For statistical reasons, five measurements of all samples were performed at each pH value and the mean value of these data was reported here.

1.7 Thermal stability measurements

The thermal stability of photosystems (PSⅠ and

PSⅡ) was studied according to the method of Liu *et al*.[6] with a Bio-logic MOS-450 circular dichroism (CD) spectrometer at different wavelengths(689 nm for PSⅠ and 682 nm for PSⅡ). The temperature was automatically controlled between 20℃ and 90℃ using a Peltier device. PSⅠ/PSⅡ sample(Chl *a* concentration was 50 mg/L) was suspended in 20 mmol/L MES buffer containing 0.07% DDM, and samples were incubated for 5 min prior to recording CD spectra using 1 mm path-length fused quartz curettes. The spectra were recorded in 1 nm steps with an integration time of 0.2 s and a band-pass of 2 nm.

1.8 Sodium dodecyl sulfate-polyacrylamide gel electrophoresis (SDS-PAGE)

The SDS-PAGE analysis was performed under reducing conditions using NuPAGE 4%～12% Bis-Tris mini gels (Invitrogen, U.S.A.), following the manufacturer's instructions. Detection of the protein bands was performed with the Brilliant Blue Coomassie G-250 staining method.

2 Results and discussion

2.1 Isolation of PSⅠ and PSⅡ from spinach

Low-temperature fluorescence emission spectra for PSⅠ/PSⅡ samples are shown in Figure 1. It can be seen that each spectrum has only one peak (PSⅠ at 725 nm and PSⅡ at 685 nm), which are characteristics of PSⅠ and PSⅡ particles[5]. The SDS-PAGE analysis (Figure 2) of the preparation showed that both PSⅠ and PSⅡ samples are in agreement well with literature results[2, 8]. The chlorophyll of PSⅠ is associated with the PsaA and PsaB polypeptides with molecular mass greater than 50 ku and a set of LHCⅠ polypeptides shown with molecular mass in the range of 20～26 ku.

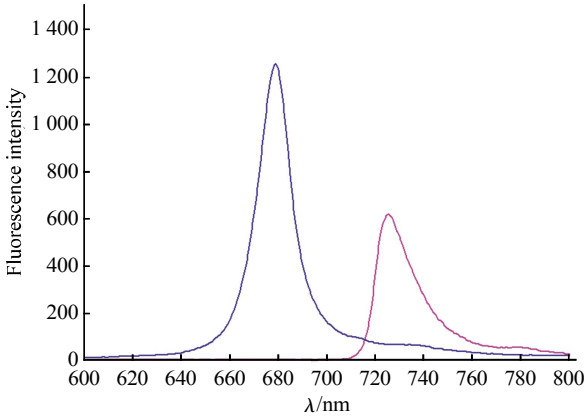

Fig. 1　Low-temperature (77 K) fluorescence emission spectra of PSⅠ and PSⅡ samples

—: PSⅠ_DDM; —: PSⅡ_DDM.

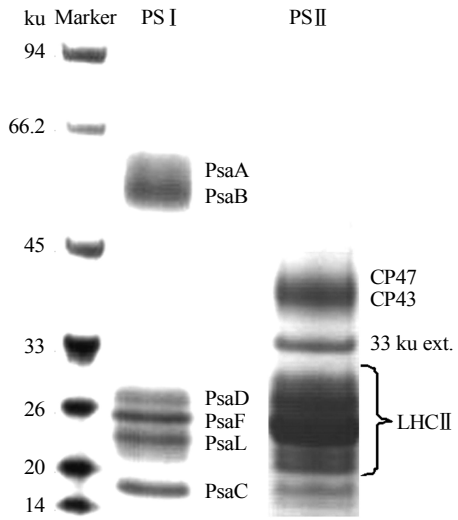

Fig. 2　SDS-PAGE analysis of prepared PSⅠ and PSⅡ samples

The PSⅡ complex consists mainly of CP47, CP43, the 33 ku extrinsic protein and a set of LHCⅡ polypeptides shown with molecular mass in the range of 23～29 ku. These results suggest that the purity of PSⅠ/PSⅡ is very high, and that no structural damage has happened[5].

2.2 Activity of PSⅠ and PSⅡ

As a systematic effort to screen the effects of solution conditions on PSⅠ/PSⅡ activities, the effect of ionic strength was examined over the sodium chloride concentration range of 0 ～ 500 mmol/L (Figure 3), covering the same concentration range previously studied for PSⅠ purification using ultrafiltration[5]. The results show that PSⅠ activity

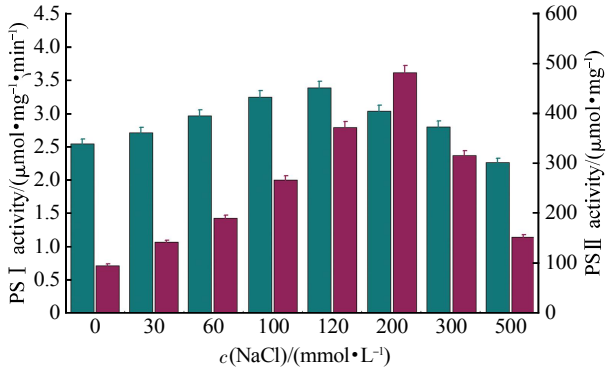

Fig. 3　Activity analysis of PSⅠ and PSⅡ samples at different sodium chloride concentrations

■: PSⅠ activity; ■: PSⅡ activity.

increases with salt concentration up to a salt concentration of 120 mmol/L. With further increase in salt concentration, the PSⅠ activity decreases. There is little data about solution ionic strength in most published papers on PSⅠ activity, and little attention has been paid to the effect of salt concentration on PSⅠ structure. However, this tendency is in good agreement with the size trend of PSⅠ aggregates as determined by AFM imaging (Figure 4), suggesting that the activity of PSⅠ may be related to its aggregation size.

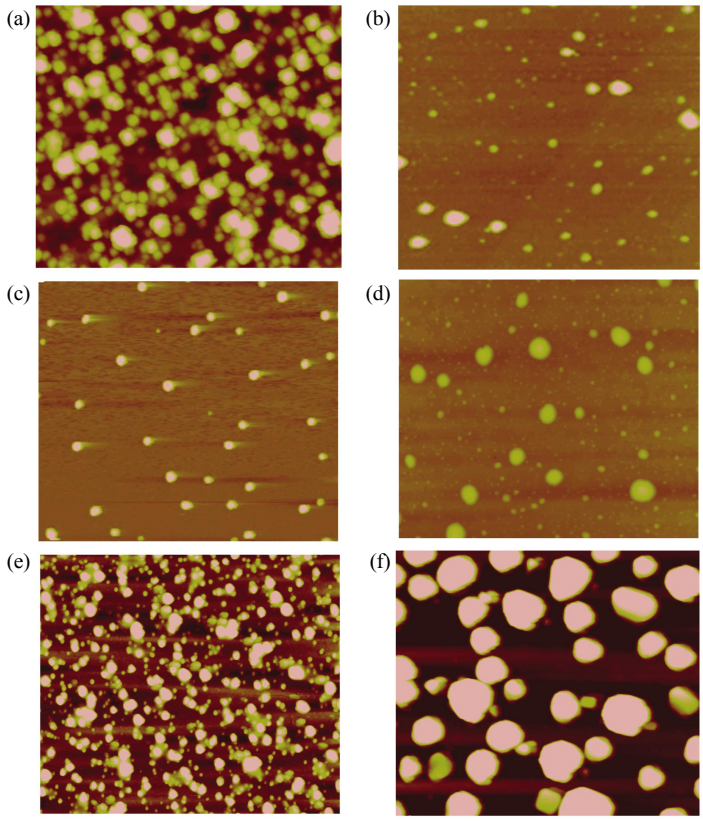

Fig. 4 AFM images of PSⅠ samples at different sodium chloride concentrations using DDM (0.07% (w/v)) as detergent
(a) 0 mmol/L NaCl. (b) 50 mmol/L NaCl. (c) 100 mmol/L NaCl. (d) 120 mmol/L NaCl. (e) 200 mmol/L NaCl. (f) 400 mmol/L NaCl.

The oxygen-evolution activity of PSⅡ follows the same trend of PSⅠ, with a maximum value at sodium chloride concentration of 200 mmol/L. The small activities of PSⅡ at lower sodium chloride concentrations (< 60 mmol/L) show that ions are necessary for PSⅡ activity measurements[9]. Another important feature of Figure 3 is that the PSⅡ activity drops rapidly when sodium chloride concentration is greater than 200 mmol/L. This may be caused by the release of the 23 ku polypeptide, which is an essential component in the oxygen evolving complex[10].

2.3 AFM imaging

The effect of ionic strength on the topological structure of PSⅠ and PSⅡ in the presence of DDM was imaged on the surface of mica using tapping mode AFM. Figure 4 shows that as sodium chloride concentration increases from 0 to 400 mmol/L, the size of PSⅠ aggregates decreases at first, but after reaching its minimum at 120 mmol/L NaCl, the size then increases. The diameters of PSⅠ aggregates at the highest activity(120 mmol/L NaCl) are from 50 to 100 nm (Figure 4c), which is very close to the reported size of PSⅠ particles in aqueous solution[11]. The calculated PSⅠ trimer has a diameter of 50 nm[12], while the PSⅠ particles in aqueous solution had a diameter between 30 and 60 nm[11], suggesting that PSⅠ from higher plants usually exists in the form of trimers or higher aggregates in solution. As for PSⅡ, the size of aggregates was not obviously altered within the studied sodium chloride concentration range. The estimated

diameters of PSⅡ aggregates at 120 mmol/L NaCl, as determined by AFM imaging, are in the range from 15 to 30 nm (Figure 5). This value is very close to the crystallographic data of PSⅡ [13].

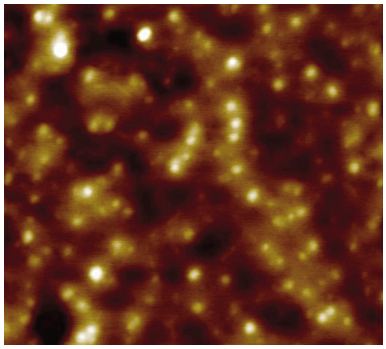

Fig. 5 AFM image of PSⅡ at 200 mmol/L NaCl using DDM (0.07% (w/v)) as detergent

2.4 Zeta potential measurements

Figure 6 shows the zeta potentials of photosystems (PSⅠ and PSⅡ) as a function of sodium chloride concentration. It can be seen that the zeta potentials of both PSⅠ and PSⅡ are negative and they increase rapidly with salt concentration up to a salt concentration of 100 mmol/L. With further increase in sodium chloride concentration, the zeta potentials of PSⅠ and PSⅡ increase slowly. Another important conclusion that can be drawn from Figure 6 is that the absolute value of PSⅡ zeta potential is greater than that of PSⅠ within the studied sodium chloride concentration range.

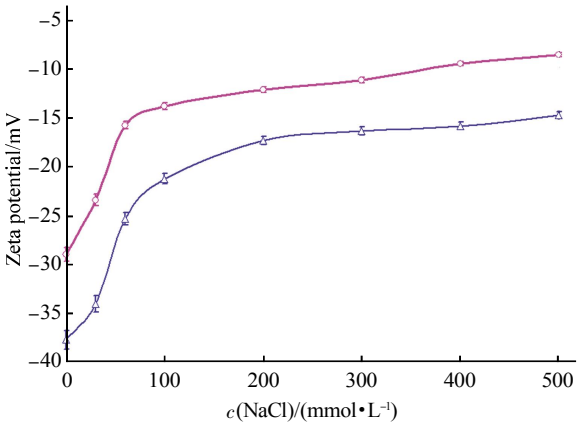

Fig. 6 Effect of sodium chloride concentration on PSⅠ and PSⅡ zeta potentials

○—○: PSⅠ_Zeta potential; △—△: PSⅡ_Zeta potential.

The zeta potential measurements were carried out at pH 10.0, which is equal to the primary optimized pH value for PSⅠ isolation using ultrafiltration[5]. This pH value is above the isoelectric points of PSⅠ (4.5～4.8)[14] and PSⅡ (4.8)[15]. Therefore, both PSⅠ and PSⅡ were negatively charged within the sodium chloride concentration range studied. In addition, PSⅠ and PSⅡ complexes became more negatively charged due to the adsorption of negative particles from solution environment at low sodium chloride concentrations. When sodium chloride concentration reached a certain value (*i.e.*, > 100 mmol/L NaCl), the zeta potential increase would be affected by the charge shielding effect.

2.5 Thermal stability

When we undertook ultrafiltration experiments for PSⅠ isolation, some precipitation appeared in the feed and retentate under some experimental conditions, which might be caused by the progressive aggregation associated with PSⅠ and/or PSⅡ unfolding and decomposition. This phenomenon was very harmful to the membrane bioseparation process as it could result in membrane fouling and blockage. Therefore, the effects of sodium chloride concentration on thermal stabilities of PSⅠ and PSⅡ were also studied in this work. The wavelengths of 689 nm and 682 nm were used to characterize the stabilities of PSⅠ and PSⅡ in the presence of DDM, which are corresponding to the largest absorption peaks of PSⅠ and PSⅡ, respectively[6].

Figure 7 shows the effect of sodium chloride concentration on thermal stability of PSⅠ. The mid-point of the change corresponds to the melting temperature [16]. As sodium chloride concentration increases from 0 to 100 mmol/L, the melting temperature of PSⅠ increases from 81 ℃ to 86 ℃, indicating that the thermal stability of PSⅠ has been improved. With further increase in sodium chloride from 100 to 400 mmol/L, the thermal stability of PSⅠ drops sharply, with the melting temperature decreasing from 86 ℃ to 76 ℃. Therefore, the highest thermal stability of PSⅠ occurred at 100 mmol/L NaCl in the presence of DDM. The thermal stability of PSⅡ follows the same trend of PSⅠ, with a maximum value at 200 mmol/L NaCl (Figure 8). These results indicate that the thermal stability of PSⅠ and PSⅡ may also be related to their aggregation sizes. Another important conclusion that can be drawn from Figure 7 and Figure 8 is that the thermal stability of PSⅠ is

higher than that of PSⅡ under experimental conditions.

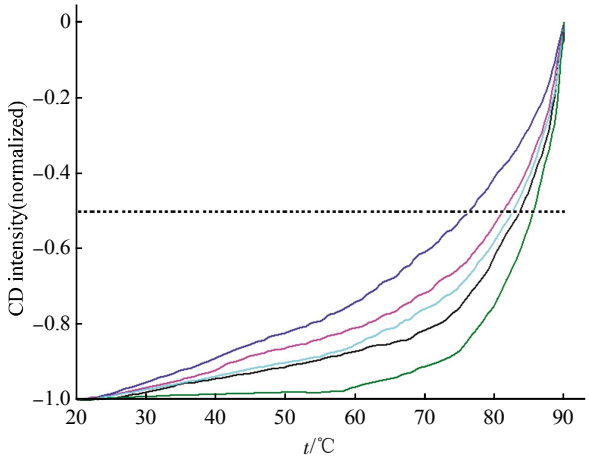

Fig. 7　Temperature dependence of CD signal of PSⅠ at 689 nm as a function of sodium chloride concentration

—: PSⅠ_NaCl_None; —: PSⅠ_NaCl_50 mmol/L; —: PSⅠ_NaCl_100 mmol/L; —: PSⅠ_NaCl_200 mmol/L; —: PSⅠ_NaCl_400 mmol/L.

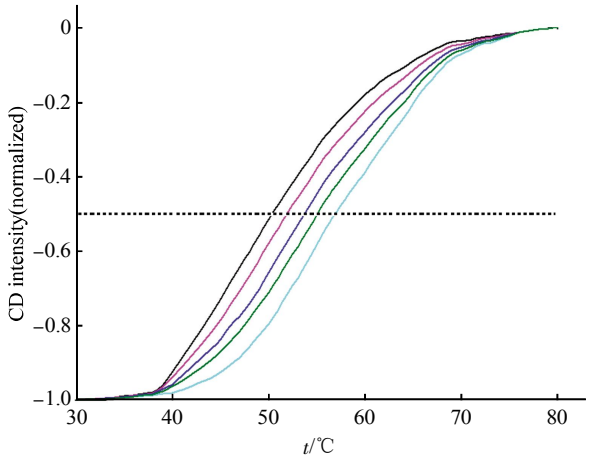

Fig. 8　Temperature dependence of CD signal of PSⅡ at 682 nm as a function of sodium chloride concentration

—: PSⅡ_NaCl_None; —: PSⅡ_NaCl_50 mmol/L; —: PSⅡ_NaCl_100 mmol/L; —: PSⅡ_NaCl_200 mmol/L; —: PSⅡ_NaCl_400 mmol/L.

2.6　Impact on PSⅠ isolation

The aim for bioseparation research is not only to obtain the target protein with high purity, but also to keep the activity and structure of target protein unchanged during the isolation process. As described in “Activity of PSⅠ and PSⅡ”, solution ionic strength was found to have a significant effect on the activity of PSⅠ and PSⅡ. In order to obtain active PSⅠ and PSⅡ simultaneously from a single-stage ultrafiltration process, more sodium chloride concentration values between 120 and 200 mmol/L should be evaluated. In addition, surfactants play a significant role in the solubilization and stabilization of membrane proteins during their purification and crystallization. Although some new surfactants have recently shown promise in the stabilization of membrane proteins[17], there are no general rules for the selection of surfactants for an individual membrane protein due to the unclear understanding of the interactions between them[16]. Therefore, the selection of surfactants to improve the stability of PSⅠ and PSⅡ, especially for PSⅡ, is the remaining task to develop a practical bioseparation process for PSⅠ isolation using ultrafiltration.

In membrane bioseparation, electrostatic interactions among the proteins and between the membrane and individual proteins affect the transmission of each protein[3]. In our previous work, the 300 ku molecular mass cut-off polyethersulfone membranes were used for PSⅠ isolation[5]. The isoelectric point of the ultrafiltration membrane is about 2.5[18], which is lower than the pH value (10.0) of the working solution used for PSⅠ isolation. Thus, both the membrane and photosystems (PSⅠ and PSⅡ) are negatively charged under operating conditions (pH 10, 0.07% DDM, 120 mmol/L NaCl)[5]. According to the “intrinsic electrostatic rejection” theory[3], the sieving coefficients of PSⅠ and PSⅡ should be very small. However, our experimental results showed that most of PSⅡ passed through the membrane. This indicates that the “molecular sieve effect” may play a central role in the newly developed ultrafiltration process for PSⅠ isolation[19]. Therefore, in order to develop a practical bioseparation process, more attention should be put on the “molecular sieve effect” for the further optimization of operating parameters.

3　Conclusions

In this work, the effects of solution ionic strength on properties of PSⅠ and PSⅡ were studied with DDM as the stabilizing detergent. The results showed that sodium chloride concentration can cast huge influence on the activity, zeta potential, aggregation size and thermal stability of PSⅠ and PSⅡ. Based on the measured zeta potentials and aggregation sizes of PSⅠ and PSⅡ, the “molecular sieve effect” was found to be the dominant mechanism for PSⅠ

purification using ultrafiltration. These results will provide theoretical guidance to make further optimization of the operating parameters for the novel membrane-based bioseparation process for PS I production.

References

[1] Ouellette A J A, Barry B A. Tandem mass spectrometric identification of spinach photosystem Ⅱ light-harvesting components. Photosynthesis Research, 2002, **72**(2): 159−173

[2] Wenk S, Kruip J. Novel, rapid purification of the membrane protein photosystem I by high-performance liquid chromatography on porous materials. Journal of Chromatograph B, 2000, **737** (1): 131−142

[3] Wang J B, Liu J G, Lu J R, *et al*. Isolation and purification of superoxide dismutase from garlic using two-stage ultrafiltration. Journal of Membrane Science, 2010, **352**(1−2): 231−238

[4] Liu J G. Effect of solution pH on partial properties of photosystem Ⅱ from spinach. Research Journal of Biotechnology, 2014, **9**(6): 81−84

[5] Liu J G, Yin M M, Wang M, *et al*. A novel membrane based process to isolate photosystem-I membrane complex from spinach. Photosynthesis Research, 2011, **107**(2):187−193

[6] Liu J G, Zhang X F, Wang M, *et al*. Characterization of photosystem I from spinach: effect of solution pH. Photosynthesis Research, 2012, **112**(1): 63−70

[7] Bruce B D, Malkin R. Subunit stoichiometry of the chloroplast photosystem I complex. Journal of Biological Chemistry, 1988, **263**(15): 7302−7308

[8] Allen K D, Staehelin L A. Biochemical characterization of photosystem Ⅱ antenna polypeptides in grana and stroma membranes of spinach. Plant Physiology, 1992, **100**(3): 1517−1526

[9] Shibata M, Kashino Y, Satoh K, *et al*. Isolation and characterization of oxygen-evolving thylakoid membranes and photosystem Ⅱ particles from a glaucocystophyte, *Cyanophora paradoxa*. Plant and Cell Physiology, 2001, **42**(7): 733−741

[10] Ljungberg U, Jansson C, Andersson B, *et al*. Reconstitution of oxygen evolution in high salt washed photosystem Ⅱ particles. Biochemical and Biophysical Research Communication, 1983, **113**(3): 738−744

[11] Matsumoto K, Zhang S G, Koutsopoulos S, *et al*. Enhanced electron transfer activity of photosystem Ⅰ by polycations in aqueous solution. Biomacromolecules, 2010, **11**(11): 3152−3157

[12] Jordan P, Fromme P, Witt H T, *et al*. Three-dimensional structure of cyanobacterial photosystem Ⅰ at 2.5Å resolution. Nature, 2001, **411**(6840): 909−917

[13] Zouni A, Witt H T, Kern J, *et al*. Crystal structure of photosystem Ⅱ from *Synechococcus elongatus* at 38Å. Nature, 2001, **409** (6821): 739−743

[14] Tamura N, Itoh S, Yamamoto Y, *et al*. Electrostatic interaction between plastocyanin and P700 in the electron transfer reaction of photosystem I-enriched particles. Plant and Cell Physiology, 1981, **22**(4): 603−612

[15] Conjeaud H, Mathis P. Electron transfer in the photosynthetic membrane: influence of pH and surface potential on the P-680 reduction kinetics. Biophysical Journal, 1986, **49**(6): 1215−1221

[16] Ge B S, Yang F, Yu D Y, *et al*. Designer amphiphilic short peptides enhance thermal stability of isolated photosystem Ⅰ. Plos One, 2010, **5**(4): 1−9

[17] Matsumoto K, Vaughn M, Bruce B D, *et al*. Designer peptide surfactants stabilize functional photosystem-I membrane complex in aqueous solution for extended time. Journal of Physical Chemistry B, 2009, **113**(1): 75−83

[18] Burns D B, Zydney A L. Contributions to electrostatic interactions on protein transport in membrane systems. AIChE Journal, 2001, **47**(5): 1101−1104

[19] Xu Y Z, Lebrun R E. Investigation of the solute separation by charged nanofiltration membrane: effect of pH, ionic strength and solute type. Journal of Membrane Science, 1999, **15**(1−2): 93−104

溶液离子强度对光系统Ⅰ和光系统Ⅱ结构性质及分离的影响*

王玲玲　黄雅琪　张学芳　曲剑波　刘建国**

(中国石油大学(华东)生物工程与技术中心，青岛 266580)

摘要　本文运用现代分析手段系统考察了溶液离子强度对菠菜来源光系统Ⅰ(PSⅠ)和光系统 (PSⅡ)结构性质的影响，研究的结构性质包括：低温荧光光谱、放(耗)氧活性、聚集尺寸、聚集形貌、Zeta 电位和热稳定性等．结果表明，溶液离子强度对PSⅠ和PSⅡ的放(耗)氧活性、聚集尺寸和热稳定性具有显著影响．此外，根据测试结果的分析得知，“筛分效应”在光系统Ⅰ的超滤分离过程中起决定性作用．

关键词　光系统Ⅰ，光系统Ⅱ，离子强度，表征，纯化

学科分类号　G633.91，K826.15，Q6　　**DOI**: 10.16476/j.pibb.2016.0006

---

* 国家自然科学基金(21276280, 21473256, 21176257)和中国石油大学研究生创新工程(YCXJ2016042)资助项目．

** 通讯联系人．

Tel: 0532-86981566, E-mail: jianguoliu@upc.edu.cn

收稿日期：2016-01-08，接受日期：2016-09-01